Sensors and Actuators B 203 (2014) 579–587

Contents lists available at ScienceDirect

Sensors and Actuators B: Chemical

journal homepage: www.elsevier.com/locate/snb

Nitrogen doped graphene and its derivatives as sensors and efficient direct electron transfer platform for enzyme biosensors

Madalina M. Barsan[a], Krishna P. Prathish[a], Xueliang Sun[b], Christopher M.A. Brett[a,*]

[a] Departamento de Química, Faculdade de Ciências e Tecnologia, Universidade de Coimbra, 3004-535 Coimbra, Portugal
[b] Department of Mechanical and Materials Engineering, The University of Western Ontario, London, Ontario, Canada N6A 5B9

ARTICLE INFO

Article history:
Received 20 March 2014
Received in revised form 25 June 2014
Accepted 7 July 2014
Available online 14 July 2014

Keywords:
Nitrogen doped graphene
Polymer composites
Ascorbate
Glucose biosensors
Xanthine and hypoxanthine sensors and biosensors

ABSTRACT

The performance of different sensor/biosensor architectures based on graphene (G), nitrogen doped graphene (NG) and their acidic/basic functionalized derivatives, as well as of polymer composites of NG have been compared, using ascorbate oxidation, and glucose enzymatic oxidation, as model reactions on glassy carbon electrode (GCE) substrates, which led to the choice of NG/GCE as the preferred modified electrode for further applications. Enzymatic and non-enzymatic sensing of hypoxanthine (Hx) and xanthine (X), two intermediates in purine metabolism, with relevance in clinical diagnostics and food chemistry, was investigated. Electrocatalytic oxidation of both Hx and X was achieved at NG/GCE, the sensor exhibiting sensitivities of 1.6 and 1.3 mA cm^{-2} mM^{-1} for Hx and X, respectively. Hx biosensing was carried out at −0.35 V vs. Ag/AgCl, the enzymatic mechanism being based on direct regeneration of FAD at NG, the analytical characteristics comparing favorably with other reported XOx biosensors. Application to the analysis of biological samples was demonstrated.

1. Introduction

Molecular recognition of biologically relevant species is of prime importance in modern clinical analysis and diagnostics, and electrochemical transducers are one of the largest group of transducers [1]. Signaling of the molecular recognition event at the electrode/solution interface can be enhanced by amplification of the chemical/physical aspects of the electrode material. Graphene (G) has shown exceptional optoelectronic and mechanical properties and due to its high surface area and excellent conductivity has numerous application potential in diverse fields such as chemical/biosensing, field effect transducers, fuel cells and supercapacitors [2–6]. Recent advances in graphene research proved that chemical doping of graphene can induce semiconductor like characteristics and the resulting *n*- or *p*-doped graphene exhibits enhanced chemical reactivity and charge conductivity [7,8]. Among the various potential dopants, nitrogen is an excellent candidate for doping the carbon framework due to its comparable size and pentavalency, so that it is able to form strong covalent bonds with carbon in nitrogen-doped graphene (NG), and it has been reported that NG is superior to G for applications in fuel cells and batteries [9–11]. In addition to the doping of heteroatoms, simple acidic/basic functionalization of doped/undoped graphene can further improve the chemico-physical properties of the material, for which we have used KOH and HNO_3 functionalized G and NG to obtain KOH_G/NG and HNO_3/G [12]. Hybrid graphene/polymer composites are yet another plausible way for tuning the properties of the graphene, with the possibility to enhance further the conductivity and electrocatalytic properties of graphene films [13].

The main metabolites of adenine nucleotide degradation in biological tissues are Hx, X and uric acid, and excessive accumulation of these metabolites in the body causes diseases such as xanthinuria, gout, perinatal asphyxia, cerebral ischemia, tumor hyperthermia, and preeclampsia, and hence the monitoring of Hx and X is important in clinical analysis [14,15]. Apart from the clinical significance, selective sensing of Hx and X has a major role in food chemistry and can give vital information on the freshness of fish foods and meat products [16]. Several analytical methods are employed for determining Hx and X, such as high performance liquid chromatography [17,18], chemiluminescence [19], and capillary electrophoresis [20]. However, portable, low cost and reliable electrochemical (bio)sensors are the best tools for real-time clinical diagnostics and food analysis. Several Hx and X sensors based on carbon nanomaterials have been reported, namely functionalized SWCNT [21], impure multi-walled carbon nanotubes (MWCNT)

* Corresponding author. Tel.: +351 239854470; fax: +351 239827703.
E-mail address: cbrett@ci.uc.pt (C.M.A. Brett).

http://dx.doi.org/10.1016/j.snb.2014.07.019
0925-4005/

[22], carbon nanofibres [23], graphitized mesoporous carbon (GMC) [24], and poly(o-aminophenol-co-pyrogallol)/reduced graphene oxide(RGO) [25]. In addition to the studies on the non-enzymatic electrocatalytic effect of NG modified electrodes toward oxidation of X and Hx, the utility of the material as a platform for immobilizing the redox active enzyme xanthine oxidase (XOx) has also been investigated. The fact that the FAD redox cofactor is located deep inside the protein matrix hinders electron transfer, and therefore biosensors require either redox mediators or nanomaterials, or both, to allow electron communication between enzyme and electrode. A few hypoxanthine biosensors based on carbon materials were reported, such as glassy carbon paste electrodes [26], MWCNT-s [27], gold nanoparticles (AuNP) with carbon nanohorns [28], and poly(styrenesulfonic acid-g-pyrrole)/reduced graphite oxide [29], others sensing xanthine only at very positive potentials, based on CNT together with AuNP [30] and CNT together with ZnO nanoparticles [31].

The present study focuses on performing a comparative evaluation of the sensing characteristics of the graphene materials, G, NG and their functionalized derivatives HNO_3_G and KOH_G/NG, as well as of some hybrid composites. The hybrid composites prepared were nitrogen doped graphene (NG) with the conducting polymer, poly(3,4-ethyleneoxythiophene) (PEDOT) or with the redox polymer, poly(neutral red) (PNR), NG_PEDOT or NG_PNR polymer composites. The sensor parameters were correlated with the electrochemical properties of all graphene materials obtained in a previous study [12]. The modified electrodes were evaluated for sensing of the model species ascorbate and glucose, after modification with glucose oxidase (GOx), in order to choose the best modifier for future applications. The best performance material, NG/GCE, was then tested for non-enzymatic and enzymatic determination of hypoxanthine (Hx) and xanthine (X), two of the uric acid precursors formed during the ATP metabolism pathway. A XOx biosensor was applied to the detection of Hx by fixed potential amperometry at −0.35 V vs. Ag/AgCl, and the stability of the biosensor was also evaluated as well as its applicability for determination of Hx in fish meat.

2. Experimental

2.1. Reagents and buffer electrolyte solutions

All reagents were of analytical grade and were used without further purification. Graphene was prepared by the oxidation of graphite powder, the dried graphite oxide being thermally reduced by heating at 1050 °C under an Ar stream. Nitrogen doped graphene was obtained by heating the graphene under high purity ammonia mixed with Ar at 900 °C [32]. Chitosan (low molecular weight), 2,3-dihydrothieno[3,4-b]-1,4-dioxin (EDOT), graphite, glutaraldehyde, neutral red (NR) 65% dye content, glucose, ascorbic acid, xanthine, hypoxanthine, monobasic and dibasic potassium phosphate, sodium chloride and sodium poly(styrene sulfonate) (NaPSS) were from Sigma–Aldrich, Germany. Potassium chloride, monobasic and dibasic sodium phosphate and the enzymes glucose oxidase, 24 U mg^{-1} (GOx) and xanthine oxidase, 0.068 U mg^{-1} (XOx) were obtained from Fluka, Switzerland.

For electrochemical experiments, the supporting electrolyte was sodium phosphate buffer saline (NaPBS) (0.1 M phosphate buffer +0.05 M NaCl, pH = 7.0). Polymerization of NR was carried out in 0.025 M potassium phosphate buffer solution plus 0.1 M KNO_3 (pH 5.5) (KPBS) containing 1 mM NR and of EDOT in 0.1 M NaPSS containing 10 mM EDOT.

Millipore Milli-Q nanopure water (resistivity ≥ 18 MΩ cm) was used for the preparation of all solutions. All experiments were performed at room temperature (25 ± 1 °C).

2.2. Instrumentation

Electrochemical experiments were performed in a three electrode cell, containing a glassy carbon electrode (GCE) (1.6 mm diameter) as working electrode, a Pt wire counter electrode and an Ag/AgCl (3.0 M KCl) reference electrode, using a μ-Autolab potentiostat/galvanostat system (Metrohm-Autolab, Netherlands).

The pH measurements were carried out with a CRISON 2001 micro pH-meter (Crison Instruments SA, Barcelona, Spain) at room temperature.

2.3. Preparation of modified electrodes and biosensors

Functionalized graphene (G) and nitrogen doped G (NG) were obtained, following the procedure described in [12], by treating either in 3 M HNO_3 or in 7 M KOH, then being thoroughly washed with Milli-Q water and dried.

Suspensions of 0.1% G, NG or their derivatives were prepared in 1% (w/v) chitosan dissolved in 1% (v/v) acetic acid [12]. The solution was sonicated for 1 h and vortexed, before 4 μl was drop cast on the GCE. The modified electrodes were left overnight to dry.

Four types of composite of NG with the conducting polymer PEDOT or the redox polymer PNR were prepared using potential cycling electropolymerisation as detailed in [12]: NG/PEDOT/GCE, PEDOT/NG/GCE, NG/PNR/GCE and PNR/NG/GCE.

For the preparation of biosensors, enzyme solutions containing bovine serum albumin (BSA) were prepared, 1% GOx + 4% BSA (24 U GOx per 100 μL enzyme solution) and 10% XOx + 10% BSA (0.68 U XOx per 100 μL enzyme solution), respectively. The enzyme solution was then mixed with GA solution 2.5%, in a volume ratio of 2:1 enzyme:GA and 2 μL of this mixture was dropped on a 1.6 mm diameter GCE, and allowed to dry for at least 4 h. Biosensors were kept in 0.1 M NaPBS pH 7.0, at 4 °C.

The preparation of such sensors and biosensors was found to be very reproducible, exhibiting sensitivities with RSD values lower than 6%, calculated for at least 3 different electrodes.

2.4. Preparation of biological samples

Intravenous glucose solution (5% glucose in serum) was purchased from a local pharmacy.

Mackerel fish was purchased from a local supermarket, the flesh divided into 2 g portions, and stored in Eppendorf containers in the refrigerator at 4 °C until use. For experiments, 2 g of fish were mixed thoroughly with 200 μL MilliQ water. After centrifugation at 4000 rpm for 30 min, the solution obtained was used for Hx determination.

3. Results and discussion

3.1. Preliminary studies to select the best graphene material for sensing/biosensing

3.1.1. Application of G, NG and derivative modified GCE as sensors for ascorbate

Ascorbic acid was selected as the model analyte to compare the efficacy of G, NG and of their derivatives, HNO_3_G and KOH_G/NG, as electrode modifiers, as well as of the NG polymer composites NG/PEDOT, PEDOT/NG, PNR/NG and NG/PNR for non-enzymatic electrocatalytic sensing. Studies using graphite were carried out in parallel for comparison.

Fig. 1 shows a CV of 1 mM ascorbic acid at bare GCE and at NG/GCE in 0.1 M NaPBS, pH 7.0. As observed, electrocatalytic oxidation of AA occurs at +0.05 V vs. Ag/AgCl at NG/GCE, with currents higher by a factor of ∼3, being 0.31 mA cm^{-2} compared with 0.11 mA cm^{-2} at +0.45 V at bare GCE. Moreover, the peak is

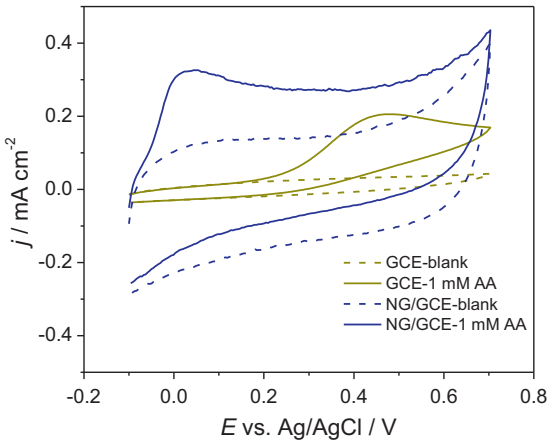

Fig. 1. Cyclic voltammograms recorded at bare GCE and modified GCE in 0.1 M NaPBS pH 7.0 and with addition of 1 mM AA; $\nu = 50\,mV\,s^{-1}$.

sharper at NG/GCE, indicating faster electron transfer kinetics. The decrease in overpotential at NG, the main advantage in using the NG/GCE, can be attributed to π–π interaction of AA with NG which lowers the charge transfer energy barrier, and the large electroactive area of the material leads to a substantial increase in current compared with bare GCE.

Since the NG and all the NG polymer composite modified electrodes showed electrocatalytic oxidation of ascorbate, all were tested as AA sensors. They all presented an AA oxidation peak that began around +0.05 V vs. Ag/AgCl. At NG/GCE, fixed potential amperometry showed that at +0.1 V the sensitivity was two times higher than at +0.05 V vs. Ag/AgCl, increasing even more at +0.2 V but, since we aimed to minimize possible interferents, +0.1 V was chosen for further measurements. A typical chronoamperometric response of the sensors is displayed in Fig. 2A, with corresponding calibration plot in Fig. 2B. The analytical performances of all sensors are shown in Table 1, and, as observed, NG/GCE showed the highest sensitivity of $337 \pm 18\,\mu A\,cm^{-2}\,mM^{-1}$ (RSD = 5.3%) among all the other tested electrodes, followed by HNO_3_G and KOH_G/NG, with sensitivities of 252 ± 13 (RSD = 5.2%), 154 ± 7 (RSD = 4.5%) and 126 ± 7 (RSD = 5.6%) $\mu A\,cm^{-2}\,mM^{-1}$ respectively, much higher than untreated graphene, which had a sensitivity of $71.8 \pm 4.6\,\mu A\,cm^{-2}\,mM^{-1}$ (RSD = 6.4%). NG/GCE also has the lowest detection limit of 0.4 μM, lower than that exhibited by other functionalized G and NG modified electrodes.

These observations are supported by the electrochemical characterization studies previously reported by our group, showing larger electroactive area and better electronic conductivities of NG, and of HNO_3_G and KOH_G/NG derivatives [12]. The electrode kinetics was found to be faster for the electroactive species $Fe(CN)_6^{3-}/Fe(CN)_6^{4-}$ at the modified electrodes. Although acidic or basic functionalization of G improved both the sensitivity and detection limit, neither was able to exceed the NG performance. However, acidic or basic functionalization of graphene both improve the hydrophilicity and the conductivity of the material, leading to more efficient substrates than undoped graphene [12].

Table 1
Analytical performance of graphene based materials modified GCE for ascorbate sensing; applied potential 0.1 V vs. Ag/AgCl, 0.1 M NaPBS pH 7.0.

Modified electrode	Sensitivity ($\mu A\,cm^{-2}\,mM^{-1}$)	LOD (μM)
Bare GCE	1.4 ± 0.1	90.0
G	71.8 ± 4.6	45.5
NG	337 ± 18	0.4
KOH_NG	126 ± 7	4.3
HNO_3_G	252 ± 13	1.5
KOH_G	154 ± 7	0.8
PEDOT/NG	111 ± 5	4.3
NG/PEDOT	103 ± 5	5.6
PNR/NG	69 ± 4	7.8
NG/PNR	113 ± 6	5.2

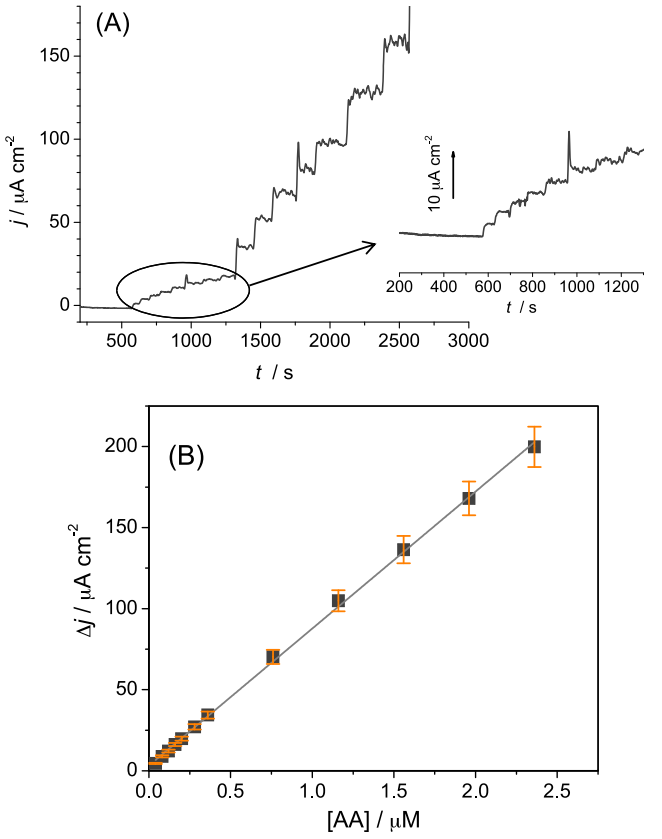

Fig. 2. (A) Typical fixed potential chronoamperogram recorded at HNO_3_G/GCE AA sensor at 0.1 V vs. Ag/AgCl in 0.1 M NaPBS, pH 7.0 and (B) corresponding calibration curve.

Composites of NG with PEDOT and PNR were also tested for ascorbate sensing to investigate whether bi-functionality has a synergistic or a detrimental effect on the sensing characteristics of the sensors. Since NG/GCE had shown the best analytical performance, these polymer composites were prepared only with NG. From Table 1 it can be seen that the polymer composites do not exhibit better analytical performance than NG, HNO_3_G or KOH_G/NG, but they are still superior to that of pure graphene (except for PNR/NG). The unexpected low sensitivities of polymer composites might be due to diffusional problems arising from thick polymer films or small film porosity. However, the polymer composites are more sensitive than the PNR [33] or PEDOT [34] modified GCE. The results prove that sp^2 hybridized NG with nitrogen in pyridinic, pyrrolic or graphitic form, is the best material for sensing applications. Hence, heteroatom doping appears to be the best way to tune the properties of graphene and so, further studies using non-enzymatic sensors were restricted to N-graphene modified GCE.

3.1.2. Application of G, NG and derivatives modified GCE as biosensors for glucose

Unlike non-enzymatic sensors, enzyme-based biosensors, although prone to instability, are highly sensitive and selective and hence a judiciously selected electrode substrate which is highly conductive, electrocatalytic and biocompatible is crucial. Thus, NG, HNO_3_G, KOH_G/NG, and NG polymer composites with PEDOT and PNR as substrates for GOx immobilization were evaluated. Comparison with HNO_3_graphite (HNO_3_Gr) was also done. Since graphite

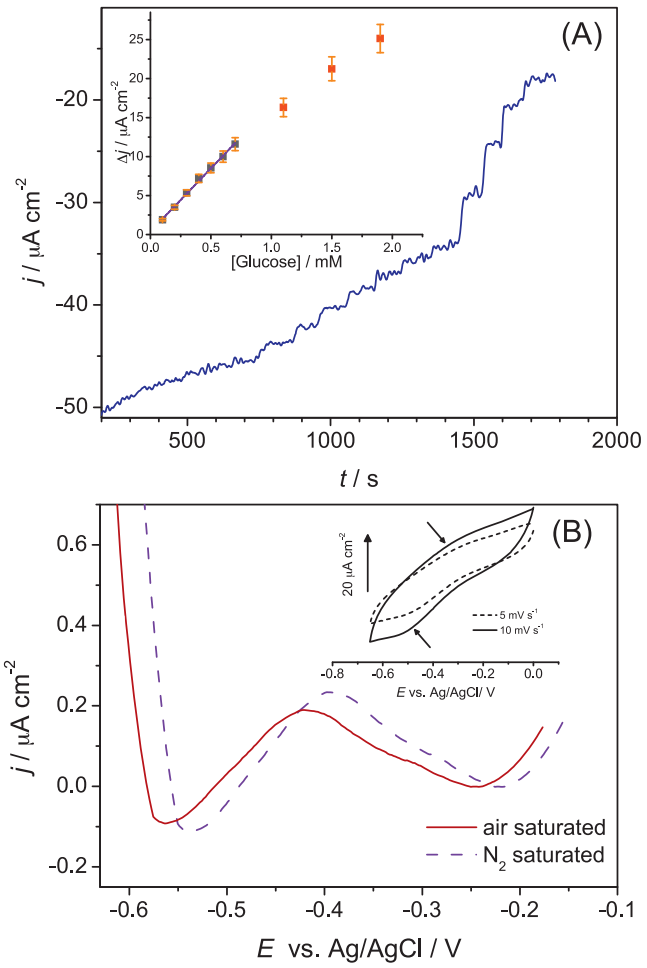

Fig. 3. (A) Typical fixed potential chronoamperogram recorded at GOx/KOH_NG/GCE at −0.35 V vs. Ag/AgCl, in inset the corresponding calibration curve; (B) DPV at GOx/NG/GCE, amplitude 50 mV, step potential 2 mV, $\nu = 5\ mV\ s^{-1}$, in inset CV of GOx/NG/GCE; all experiments done in 0.1 M NaPBS, pH 7.0.

is the starting material for the synthesis of graphene, this helps in understanding the variation in electrochemical and analytical parameters between the graphite and graphene materials.

All the biosensors developed were used for the chronoamperometric detection of glucose in 0.1 M NaPBS, pH 7.0 at an applied potential of −0.35 V vs. Ag/AgCl, which is well below the oxidation potential of many of the expected interfering species such as ascorbate, dopamine, uric acid etc. Previously, we had shown the electrocatalytic effect of NG and KOH_NG on the regeneration of the enzyme cofactors FAD and NAD [12]. A sharp reversible redox couple corresponding to FAD/$FADH_2$ (midpoint potential of −0.43 V) was observed, with greatly enhanced current (∼ 40 fold) at NG/GCE compared to bare GCE, which motivated studying the possibility of direct electron transfer from glucose oxidase, where the FAD redox system is embedded deep inside the protein scaffold.

A typical chronoamperometric response of a GOx biosensor is presented in Fig. 3, with the corresponding calibration plot in the inset, and as observed, an oxidative change in current was recorded upon glucose injection.

Cyclic voltammograms recorded at GOx/NG/GCE in 0.1 M NaPBS pH 7.0 reveal a pair of redox peaks with midpoint potential of ∼ −0.40 V vs. Ag/AgCl and a peak to peak separation of 100 mV (not shown), indicating that the redox cofactor of the enzyme, FAD, is reduced to $FADH_2$ and then quasi-reversibly re-oxidized to FAD. Better defined peaks were obtained in DPV measurements

Table 2
Analytical performance of glucose biosensors based on graphene materials modified GCE for; applied potential −0.35 V vs. Ag/AgCl, 0.1 M NaPBS pH 7.0.

Modified electrode	Sensitivity ($\mu A\ cm^{-2}\ mM^{-1}$)	LOD (μM)
Bare GCE	0.7 ± 0.1	50.6
HNO_3_graphite	2.7 ± 0.2	22.8
NG	12.8 ± 0.4	17.0
KOH_NG	12.8 ± 0.4	23.9
HNO_3_G	12.8 ± 0.4	20.0
KOH_G	12.8 ± 0.4	13.0
PEDOT/NG	8.5 ± 0.8	24.2
NG/PEDOT	8.5 ± 0.8	22.9
PNR/NG	0.6 ± 0.1	60.9
NG/PNR	0.6 ± 0.1	55.3

performed at GOx/NG/GCE in 0.1 M NaPBS pH 7.0, air and N_2-saturated, revealed an oxidation peak at ∼−0.40 and −0.43 V vs. Ag/AgCl, respectively, of roughly the same height, corresponding to the redox reaction of the cofactor, the peak potential being slightly more positive in the absence of O_2.

Fixed potential chronamperograms in buffer solution without oxygen (saturated with N_2) and in air-saturated buffer, revealed that biosensor sensitivity is a factor of two lower in the absence of O_2, supported by the fact that enzyme activity is highest when O_2 present, since the GOx is from the highly aerobic species *Aspergillus niger*.

Since the currents recorded were always oxidation currents, and taking into account CV and DPV measurements, it can be deduced that the mechanism involves direct regeneration of FAD, according to:

$$\text{Glucose} + \text{GOx(FAD)} \rightarrow \text{Gluconolactone} + \text{GOx}(FADH_2)$$

$$\text{GOx}(FADH_2) \rightarrow \text{GOx(FAD)} + 2e^- + 2H^+$$

It may be that the electrostatic interaction between negatively charged enzyme and positively charged chitosan layer containing the NG nanoparticles shortens the distance between enzyme and NG, enabling direct electron transfer from the enzyme cofactor, similarly observed in [35].

The sensitivities and LODs for each of the modified electrodes for glucose sensing are given in Table 2. As observed, modification by any of graphene derivatives leads to a substantial increase in sensitivity and decrease of detection limit values, compared to those obtained at bare electrodes modified with enzyme. Among the various modified electrodes, the sensitivities of NG, HNO_3_G and KOH_G/NG were found to be in the same range of ∼12.0–13.0 $\mu A\ cm^{-2}\ mM^{-1}$, with the lowest detection limit of 13.0 μM for KOH_G and the highest for KOH_NG, of 23.9 μM. The dynamic working ranges of all types of modified electrode were found to be up to 1.2 mM. The enzymatic sensing characteristics of acidic/basic functionalized G/NG were very similar to NG, unlike non-enzymatic ascorbate sensing, where large differences were observed, see Section 3.1.1. Hence, it can be concluded that NG, HNO_3_G and KOH_G/NG are equally good candidates for enzyme biosensing, although functionalized graphene is a good alternative to NG in situations where synthesizing or acquiring NG is difficult.

The efficiency of NG-based conducting/redox polymer composites toward glucose biosensing was also tested. Sensing features of PEDOT/NG and NG/PEDOT were very similar, but slightly inferior compared to NG, with sensitivity of 8.5 ± 0.8 $\mu A\ cm^{-2}\ mM^{-1}$ and detection limits of 29 ± 6 μM. Sensitivities of PNR/NG and NG/PNR modified GCEs were well below that of NG, probably due to diffusional problems, which need to be further investigated. The results indicate that too many components on the electrode surface, in this case the presence of redox or conducting polymers, do not improve NG performance.

Table 3
Recently reported carbon nanomaterial based sensors for Hx and X and biosensors for Hx.

Electrode	Sensitivity ($\mu A\,cm^{-2}\,mM^{-1}$)	LOD (nM)	Reference
Hx and X sensors			
Functionalized SWCNT	Hx: 0.68 X: 0.26	Hx: 560 X: 146	[21]
Impure MWCNT	Hx: 1832 X: 637.9	Hx: 287 X: 134	[22]
Carbon nanofibres	X: 364.0	X: 500	[23]
Graphitized mesoporous carbon	Hx: 1594 X: 872.7	Hx: 351 X: 388	[24]
Poly(o-aminophenol-co-pyrogallol)/RGO[a]	X: 2357	X: –	[25]
NG/GCE	Hx: 1577 X: 1264	Hx: 470 X: 250	This work
Hx biosensors			
GCPE[b] (+0.90 V)	17.0	5300	[26]
MWCNT (−0.30 V)	23.3	750	[27]
AuNP[c]/carbon nanohorns (+0.40 V)	202.4	610	[28]
PSSA-g-PPY[d]/RGO[a] (+0.55 V)	0.7	10	[29]
XOx/NG/GCE (−0.35 V)	135.6	180	This work

[a] Reduced graphite oxide.
[b] Glassy carbon paste electrode.
[c] Gold nanoparticles.
[d] Poly(styrenesulfonic acid-g-pyrrole).

3.1.3. Determination of glucose in intravenous sugar solution

The intravenous sugar solution, 5% glucose in serum, was diluted in MilliQ water to obtain 0.1 M glucose and used as a glucose sample, injecting 10 μL aliquots into 10 mL of 0.1 M NaPBS solution, pH 7.0, at −0.35 V vs. Ag/AgCl. The GOx/NG/GCE biosensor detected 5.44 g glucose per 100 ml solution, slightly lower than the 5.50 g per 100 ml solution, declared by the producer, using the standard addition method, the precision being 98.9%. Moreover, calibration curves were recorded by using 0.1 M glucose standard or 0.1 M intravenous sugar solution, the sensitivity and detection limit of the biosensor having the same values. Calculated recovery factors were between 98.5 and 100.3%, underlying the reliability of the glucose biosensor as an analytical tool.

3.2. Electrocatalytic oxidation of Hx and X at NG/GCE

The electrocatalytic oxidation of Hx and X at NG/GCE was investigated using differential pulse voltammetry (DPV). The DPV parameters that led to the best-defined DPV peaks were: increment 2 mV, amplitude 100 mV, and scan rate 10 mV s^{-1}. Interestingly, variations in the Hx peak currents toward more positive potentials upon increase in the analyte concentrations were noticed, also observed in [24], which suggests the possible existence of an EC′ mechanism that needs to be explored in the future. NG exhibited electrocatalytic activity toward both Hx and X oxidation, lowering the Hx and X oxidation potentials from +1.06 V and +0.69 V at bare GCE to +0.88 V and +0.56 V vs. Ag/AgCl respectively, with a simultaneous substantial increase in the peak currents (see Fig. 4), by a factor of more than 10 for Hx (36.4–391 $\mu A\,cm^{-2}\,mM^{-1}$) and nearly 20 for X (26.3–488 $\mu A\,cm^{-2}\,mM^{-1}$). This underlines the suitability of NG for detection of both Hx and X.

The effect of solution pH on DPV response for Hx and X was evaluated, in the pH range from 5 to 12, Fig. 5a and b, respectively. The peak potentials systematically decreased with increasing solution pH by 60 and 54 mV/pH unit for Hx and X, respectively, close to the

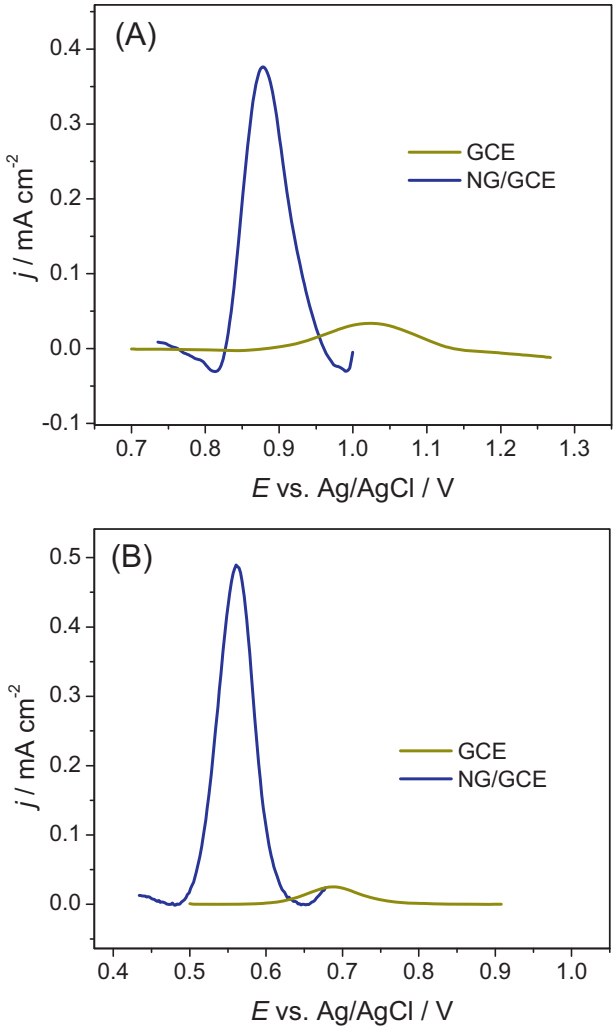

Fig. 4. DPVs recorded at GCE and NG/GCE in 0.1 M NaPBS pH 7.0 in the presence of 0.4 mM of (A) Hx and (B) X; amplitude 100 mV, step potential 2 mV, $\nu = 10$ mV s^{-1}.

Nernstian slope value of 59 mV/pH for an equal number of electrons and protons involved in the electrochemical reaction. From the DPV data of Fig. 4, the measured peak-width at half height ($W_{1/2}$) for the Hx oxidation peak is 85 mV, while for X it is 50 mV, suggesting a mechanism involving two electrons and two protons for both Hx and X, as presented in Scheme 1 and in agreement with [36,37], being kinetically slower for Hx. The pH also had an influence on the peak current for both Hx and X, increasing from pH 5 to 7 for Hx and to 6 for X, then decreasing at higher pH. Taking this into account, pH 7 was chosen for further measurements.

DPV scans, under the optimized conditions, are displayed in Fig. 6a and b for Hx and X respectively, with the corresponding calibration plots in the insets. The sensor revealed a linear increase in the oxidation current signals up to 0.7 mM, for both Hx and X.

The sensitivity of NG/GCE was slightly higher for Hx, $1577 \pm 99\ \mu A\,cm^{-2}\,mM^{-1}$ (RSD 6.2%) and for X of $1264 \pm 78\ \mu A\,cm^{-2}\,mM^{-1}$ (RSD 6.1%). Higher sensitivities for Hx compared to X were also reported for previous Hx, X electrochemical sensors [21,22,24], see Table 3. The calculated detection limit value, following the 3 × SD/slope criterion, was 0.5 μM for Hx and 0.3 μM for X, comparable with previously reported ones [21–24].

Sensitivity toward Hx was much higher than reported for functionalized SWCNT [21], very close to that exhibited by graphitized

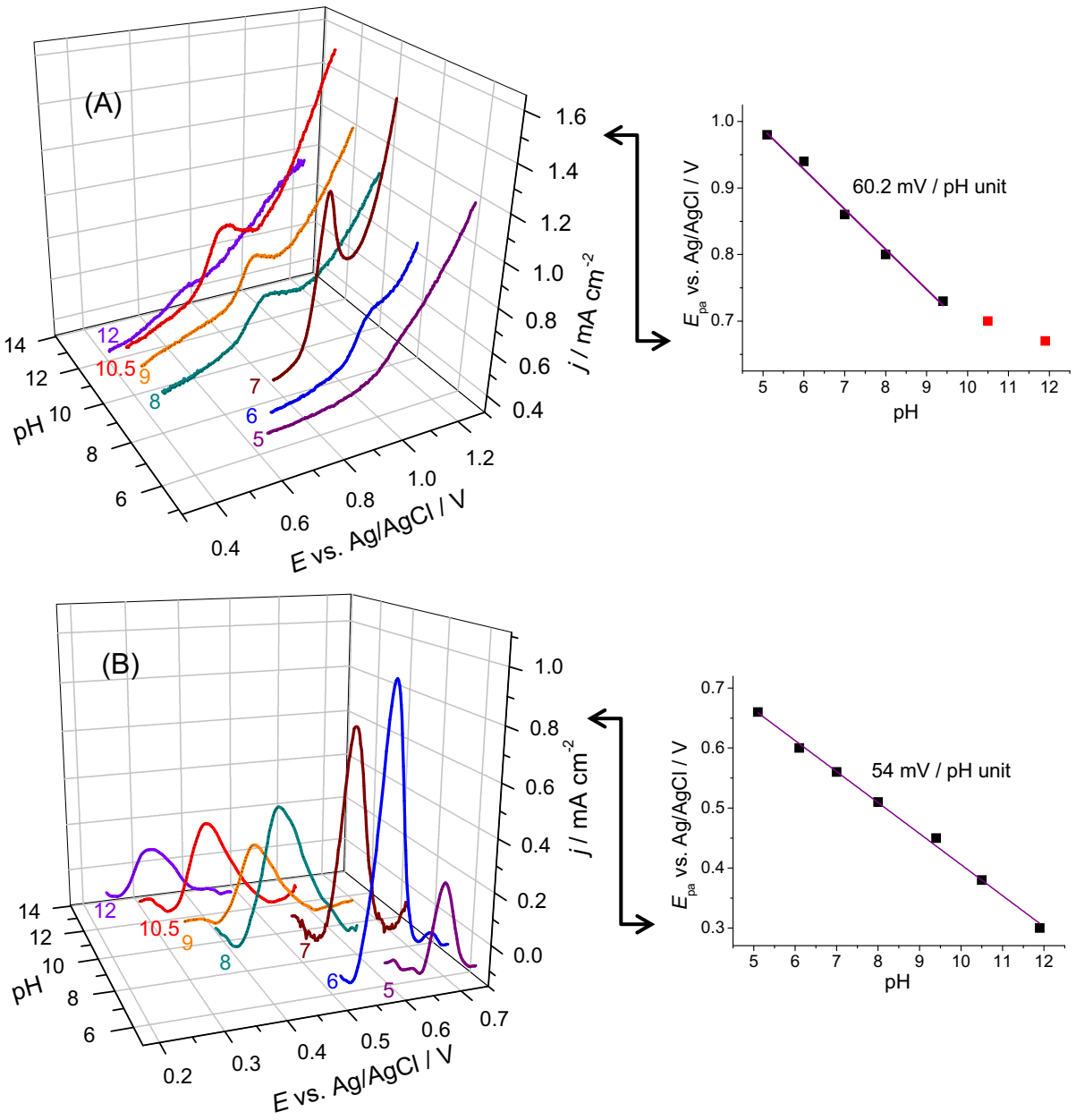

Fig. 5. Effect of pH on DPV response of (A) Hx and (B) X and corresponding plots of E_{pa} vs. pH.

mesoporous carbon [24] and just slightly lower than impure MWCNT [22]. However, the sensitivity toward X was higher than most reported sensors [21–24], lower only than the sensor reported in [25], based on poly(o-aminophenol-co-pyrogallol)/RGO.

No interferences were observed from dopamine, uric acid or ascorbate, their oxidation potentials being less positive at NG/GCE.

3.3. Analytical performance of the XOx/NG/GCE biosensor

The NG modified GCE was used as substrate to construct an amperometric xanthine oxidase enzyme biosensor for hypoxanthine. The optimum values selected for the pH (between 5.0 and 8.0) and applied potential (between −0.4 and +0.2 V vs. Ag/AgCl)

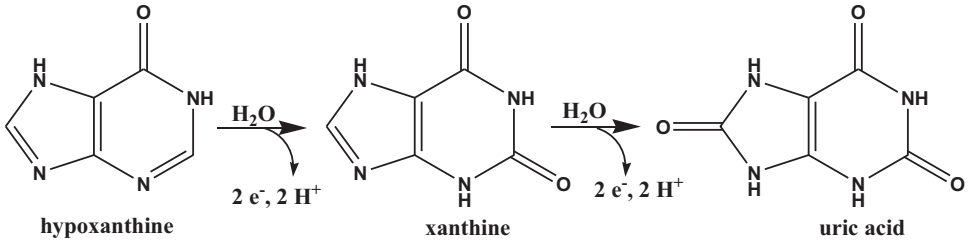

Scheme 1. Oxidation reaction mechanism for hypoxanthine and xanthine.

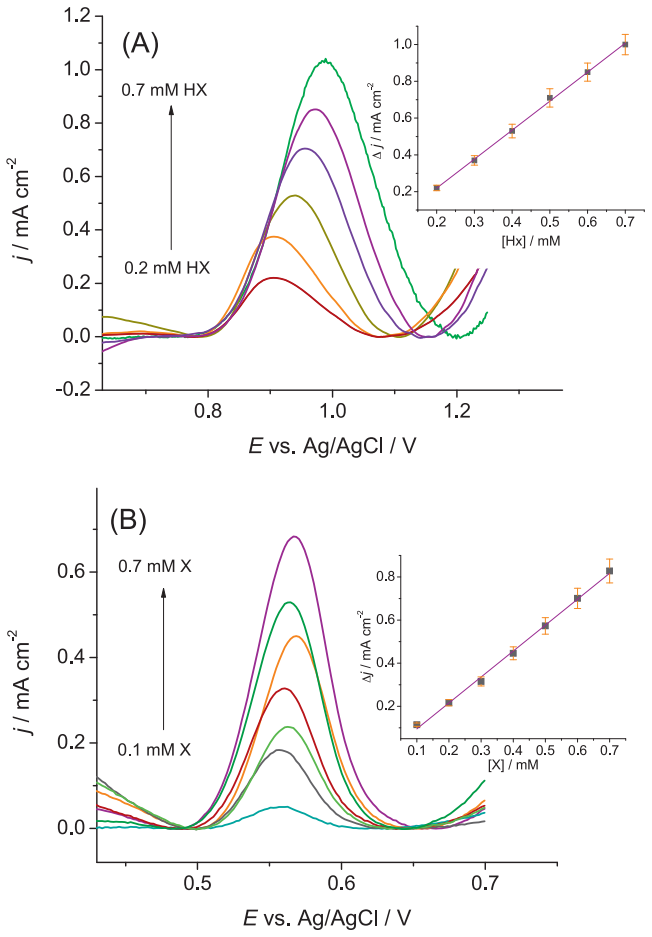

Fig. 6. DPVs at NG/GCE in 0.1 M NaPBS pH 7.0 for increasing concentrations of (A) Hx and (B) X; insets are corresponding calibration plots; amplitude 100 mV, step potential 2 mV, $v = 10\,mV\,s^{-1}$.

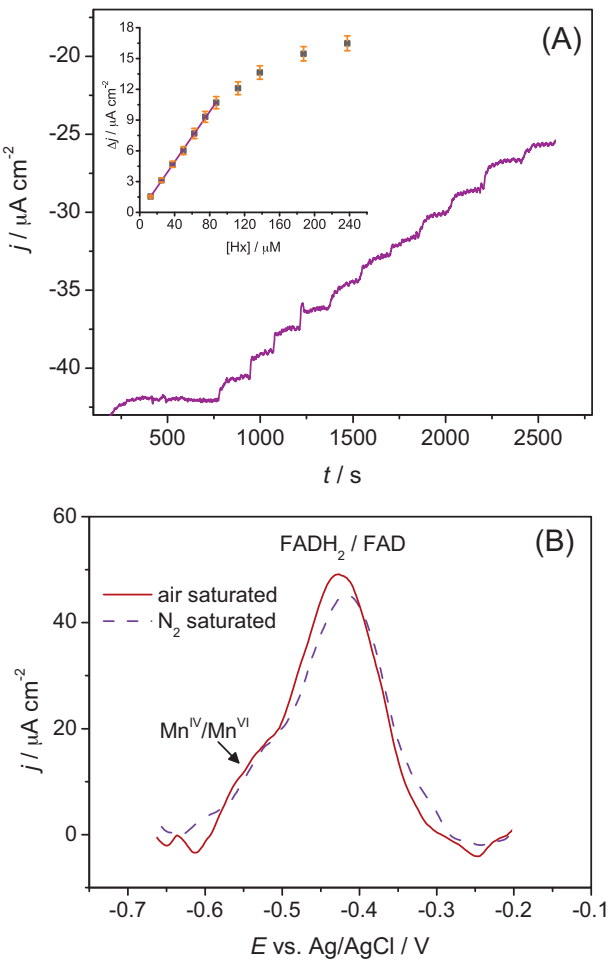

Fig. 7. (A) Typical fixed potential chronoamperogram recorded at XOx/NG/GCE for increasing concentrations of Hx at −0.35 V vs. Ag/AgCl in 0.1 M NaPBS, pH 7.0 and in inset the corresponding calibration curve; (B) DPV at XOx/NG/GCE in 0.1 M NaPBS, pH 7.0, amplitude 50 mV, step potential 2 mV, $v = 5\,mV\,s^{-1}$.

were determined by comparing biosensor response to 80 μM Hx and X (not shown), which led to the choice of pH 7.0 and a detection potential value of –0.35 V vs Ag/AgCl. At this potential we expect elimination of, or very little, interferences from other electrochemically active compounds. In the potential interval tested, the biosensor did not show any response to X, being very selective for Hx at potentials more negative than −0.2 V vs. Ag/AgCl. Previously reported XOx biosensors that sensed X, all required positive potentials above +0.4 V [26,28,30,31], and since non-enzymatic NG/GCE xanthine detection exhibited very good analytical characteristics, detecting X at +0.56 V by DPV, without interferences from dopamine, uric acid and ascorbate, there is little interest in using a biosensor for detection of X. Moreover, there will be a cumulative response from enzymatic and non-enzymatic processes, at higher potentials resulting in anomalously high sensitivities due to a combination of enzymatic and non-enzymatic processes.

A typical chronoamperometric response of the XOx/NG/GCE biosensor to Hx is presented in Fig. 7A, with the corresponding calibration plot in the inset. The linear range was up to 100 μM Hx, and the sensor exhibited a sensitivity of $126 \pm 8\,\mu A\,cm^{-2}\,mM^{-1}$ (RSD 6.5%) and achieved a detection limit of 0.18 ± 0.02 (RSD 11%) μM, calculated according to the 3 × SD/slope criterion.

One of the important features of the present biosensor is that it can operate at −0.35 V vs. Ag/AgCl, the enzyme mechanism being based on the direct cofactor regeneration at NG. Like other known molybdenum-containing oxidoreductases, the oxygen atom supplied to the substrate by XOx originates from water rather than from dissolved oxygen (O_2) [38]. The redox reaction centers are almost linearly positioned in the order of molybdoprotein, two [2Fe-2S] type iron sulfur centers and FAD. The enzyme catalyses an oxidative hydroxylation reaction, in which 2 electrons are withdrawn from the substrate to the molybdenum during the hydroxylation reaction, and are then transferred to FAD via the iron sulfur centers [39]. Finally, a $FADH_2$ oxidizes transferring the electrons to a final electron acceptor, which here is the electrode as shown in Scheme 2, and evidenced by the DPV curves recorded at XOx/NG/GCE, shown in Fig. 7B. Net oxidation currents of $FADH_2$ are recorded around −0.42 V vs. Ag/AgCl, in both air and N_2-saturated solutions, having approximately the same values.

Beside the MWCNT biosensor [27], all other XOx biosensors operate at high positive potentials between +0.4 and +0.9 V, the oxidation of H_2O_2 produced by the enzymatic reaction being monitored [26,28–31]. Even so, the biosensor had higher sensitivities than most Hx biosensors [26,27,29], Table 3, except for the one based on AuNP/carbon nanohorns [28]. The detection limit was also lower than most reported, only the one in [29] being lower.

No interferences were observed at −0.35 V vs. Ag/AgCl from ascorbate, uric acid or dopamine, for the concentration ratio 2:1 interfering compound:Hx.

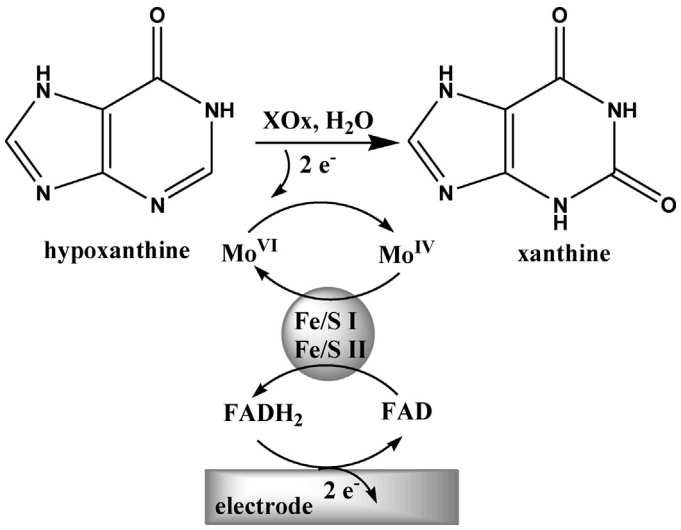

Scheme 2. Oxidation reaction mechanism of hypoxanthine by xanthine oxidase.

Table 4
Determination of Hx in fish extract solutions, stored during different periods of time, using the XOx/NG/GCE biosensor.

Days of storage	Added Hx (μM)	Found Hx (μM)	Recovery (%)
2	0	3.5	–
	15	19.0	102.7
	30	32.9	98.2
	45	47.4	97.7
5	0	8.0	–
	15	23.7	103.0
	30	37.4	98.4
	45	52.5	99.1
6	0	10.0	–
	15	25.3	101.2
	30	39.6	99.0
	45	54.1	98.4
7	0	10.0	–
	15	25.4	101.6
	30	39.5	98.8
	45	54.3	98.7

3.4. Determination of Hx in biological samples using the XOx/NG/GCE biosensor

The standard addition method was used to determine the Hx concentration in mackerel fish solution extracts, using the XOx/NG/GCE biosensor at −0.35 V vs. AgAgCl. In order to follow the increase in Hx concentration in fish meat with time, samples stored in the refrigerator during different time periods were analyzed, prepared as described in Section 2.4, injecting 10 μL aliquots into 10 mL of 0.1 M NaPBS, pH 7.0. Results obtained are presented in Table 4, together with recovery factors. As expected, the Hx concentration increased with time of storage of the fish sample, from 36 mg per 100 g of fish, detected in the second day, to 82 mg, in the fifth day and 103 mg per 100 g of fish meat, for sixth and seventh day of storage, respectively. The values are in agreement with previously reported ones [40]. The recovery factors close to 100% (see Table 4) demonstrate that the Hx biosensor is suitable for Hx determination in biological samples.

4. Conclusions

Glassy carbon electrodes modified with graphene (G), nitrogen doped graphene (NG) or their acidic/basic functionalized derivatives have been tested for application in enzymatic and non-enzymatic (bio)sensing. Non-enzymatic sensing of the model analyte ascorbate was better at NG, while acidic/basic functionalized G and NG were equally as good as NG for glucose enzymatic sensing. NG exhibited an electrocatalytic effect toward oxidation of both X and Hx, decreasing their oxidation potentials, with a simultaneous substantial increase in the peak currents. Under the optimized DPV conditions, the sensor revealed sensitivities of 1.6 and 1.3 mA cm^{-2} mM^{-1}, for Hx and X, respectively, higher than most reported in the literature. A xanthine oxidase NG based biosensor was also developed and applied for the determination of HX, an important feature of the present biosensor being operability at −0.35 V vs. Ag/AgCl, with an enzyme mechanism based on direct cofactor regeneration at NG. The biosensor showed higher sensitivities than most carbon nanomaterial-based Hx biosensors, that all operate at higher potentials, the response being free of interferences from ascorbate, uric acid and dopamine. Both GOx and XOx based biosensors were used successfully for the determination of glucose and hypoxanthine, respectively, in biological samples.

Acknowledgements

Financial support from Fundação para a Ciência e a Tecnologia (FCT), Portugal, PTDC/QUI-QUI/116091/2009, POCH, POFC-QREN (co-financed by FSE and European Community FEDER funds through the program COMPETE – Programa Operacional Factores de Competitividade under the projects PEst-C/EME/UI0285/2013 and CENTRO -07-0224 -FEDER -002001 (MT4MOBI)) is gratefully acknowledged. M.M.B. and K.P.P. thank FCT for postdoctoral fellowships SFRH/BPD/72656/2010 and SFRH/BPD/78939/2011.

References

[1] J. Janata, Principles of Chemical Sensors, 2nd edition, 2008, pp. 99–118 (Chapter 6).
[2] D. Usachov, O. Vilkov, A. Grüneis, D. Haberer, A. Fedorov, V.K. Adamchuk, A.B. Preobrajenski, P. Dudin, A. Barinov, M. Oehzelt, C. Laubschat, D.V. Vyalikh, Nitrogen-doped graphene: efficient growth, structure, and electronic properties, Nano Lett. 11 (2011) 5401–5417.
[3] R. Lv, M. Terrones, Towards new graphene materials: doped graphene sheets and nanoribbons, Mater. Lett. 78 (2012) 209–218.
[4] H. Liu, Y. Liu, D. Zhu, Chemical doping of graphene, J. Mater. Chem. 21 (2011) 3335–3345.
[5] Y. Xin, J. Liu, X. Jie, W. Liu, F. Liu, Y. Yin, J. Gu, Z. Zou, Preparation and electrochemical characterisation of nitrogen doped graphene by microwave as supporting materials for fuel cell catalysts, Electrochim. Acta 60 (2012) 354–358.
[6] S. Yang, L. Zhi, K. Tang, X. Feng, J. Maier, K. Müllen, Efficient synthesis of heteroatom (N or S)-doped graphene based on ultrathin graphene oxide-porous silica sheets for oxygen reduction reactions, Adv. Funct. Mater. 22 (2012) 3634–3640.
[7] L. Zhao, R. He, K.T. Rim, T. Schiros, K.S. Kim, H. Zhou, C. Gutiérrez, S.P. Chockalingam, C.J. Arguello, L. Palova, D. Nordlund, M.S. Hybertsen, D.R. Reichman, T.F. Heinz, P. Kim, A. Pinczuk, G.W. Flyn, A.M. Pasupathy, Visualizing individual nitrogen dopants in monolayer graphene, Science 133 (2011) 998–1003.
[8] T. Schiros, D. Nordlund, L. Pálová, D. Prezzi, L. Zhao, K.S. Kim, U. Wurstbauer, C. Gutiérrez, D. Delongchamp, C. Jaye, D. Fischer, H. Ogasawara, L.G.M. Pettersson, D.R. Reichman, P. Kim, M.S. Hybertsen, A.N. Pasupathy, Connecting dopant bond type with electronic structure in n-doped graphene, Nano Lett. 12 (2012) 4025–4031.
[9] D. Geng, Y. Chen, Y. Chen, Y. Li, R. Li, X. Sun, S. Ye, S. Knights, High oxygen-reduction activity and durability of nitrogen-doped graphene, Energy Environ. Sci. 4 (2011) 760–764.
[10] X. Li, D. Geng, Y. Zhang, X. Meng, R. Li, X. Sun, Superior cycle stability of nitrogen-doped graphene nanosheets as anode for lithium ion batteries, Electrochem. Commun. 13 (2011) 822–825.
[11] Y. Li, J. Wang, X. Li, D. Geng, M. Banis, R. Li, X. Sun, Nitrogen-doped graphene nanosheets as cathode materials with excellent electrocatalytic activity for high capacity lithium-oxygen batteries, Electrochem. Commun. 18 (2012) 12–15.
[12] K.P. Prathish, M.M. Barsan, D. Geng, X. Sun, C.M.A. Brett, Chemically modified graphene and nitrogen-doped graphene: electrochemical characterisation and sensing applications, Electrochim. Acta 114 (2013) 533–542.
[13] A.Y.W. Shama, S.M. Notley, A review of fundamental properties and applications of polymer–graphene hybrid materials, Soft Matter 9 (2013) 6645–6653.
[14] K. Safranow, Z. Machoy, J. Chromatogr. B: Analyt. Technol. Biomed. Life Sci. 819 (2005) 229–235.

[15] A.A. Ejaz, W. Mu, D.H. Kang, C. Roncal, Y.Y. Sautin, G. Henderson, I. Tabah-Fisch, B. Keller, T.M. Beaver, T. Nakagawa, R.J. Johnson, Could uric acid have a role in acute renal failure? Clin. J. Am. Soc. Nephrol. 2 (2007) 16–21.
[16] J.H.T. Luong, K.B. Male, A.L. Nguyen, Application of polarography for monitoring the fish postmortem metabolite transformation, Enzyme Microb. Technol. 11 (1989) 277–282.
[17] N. Cooper, R. Khosravan, C. Erdmann, J. Fiene, J.W. Lee, Quantification of uric acid, xanthine and hypoxanthine in human serum by HPLC for pharmacodynamic studies, J. Chromatogr. B 837 (2006) 1–10.
[18] M. Huang, J. Gao, Z. Zhai, Q. Liang, Y. Wang, Y. Bai, G. Luo, An HPLC–ESI-MS method for simultaneous determination of fourteen metabolites of promethazine and caffeine and its application to pharmacokinetic study of the combination therapy against motion sickness, J. Pharm. Biomed. Anal. 62 (2012) 119–128.
[19] J. Hlavay, S.D. Haemmerli, G.G. Guilbault, Fibre-optic biosensor for hypoxanthine and xanthine based on a chemiluminescence reaction, Biosens. Bioelectron. 9 (1994) 189–195.
[20] E. Caussé, A. Pradelles, B. Dirat, A. Negre-Salvayre, R. Salvayre, F. Couderc, Simultaneous determination of allantoin, hypoxanthine, xanthine, and uric acid in serum/plasma by CE, Electrophoresis 28 (2007) 381–387.
[21] Z. Wang, X. Dong, J. Li, An inlaying ultra-thin carbon paste electrode modified with functional single-wall carbon nanotubes for simultaneous determination of three purine derivatives, Sens. Actuators B 131 (2008) 411–416.
[22] A.S. Kumar, R. Shanmugam, Simple method for simultaneous detection of uric acid, xanthine and hypoxanthine in fish samples using a glassy carbon electrode modified with as commercially received multiwalled carbon nanotubes, Anal. Methods 3 (2011) 2088–2094.
[23] X. Tang, Y. Liu, H. Hou, T. You, A nonenzymatic sensor for xanthine based on electrospun carbon nanofibers modified electrode, Talanta 83 (2011) 1410–1414.
[24] R. Thangaraj, A.S. Kumar, Graphitized mesoporous carbon modified glassy carbon electrode for selective sensing of xanthine, hypoxanthine and uric acid, Anal. Methods 4 (2012) 2162–2171.
[25] S. Mu, Q. Shi, Xanthine biosensor based on the direct oxidation of xanthine at an electrogenerated oligomer film, Biosens. Bioelectron. 47 (2013) 429–435.
[26] Ü.A. Kirgöz, S. Timur, J. Wang, A. Telefoncu, Xanthine oxidase modified glassy carbon paste electrode, Electrochem. Commun. 6 (2004) 913–916.
[27] A.C. Torres, M.E. Ghica, C.M.A. Brett, Design of a new hypoxanthine biosensor: xanthine oxidase modified carbon film and multi-walled carbon nanotube/carbon film electrodes, Anal. Bioanal. Chem. 405 (2013) 3813–3822.
[28] L. Zhang, J. Lei, J. Zhang, L. Ding, H. Ju, Amperometric detection of hypoxanthine and xanthine by enzymatic amplification using a gold nanoparticles–carbon nanohorn hybrid as the carrier, Analyst 137 (2012) 3126–3131.
[29] J. Zhang, J. Lei, R. pan, Y. Xue, H. Ju, Highly sensitive electrocatalytic biosensing of hypoxanthine based on functionalization of graphene sheets with water-soluble conducting graft copolymer, Biosens. Bioelectron. 26 (2010) 371–376.
[30] R. Villalonga, P. Díez, M. Eguílaz, P. Martínez, J.M. Pingarrón, Supramolecular immobilization of xanthine oxidase on electropolymerized matrix of functionalized hybrid gold nanoparticles/single-walled carbon nanotubes for the preparation of electrochemical biosensors, Appl. Mater. Interfaces 4 (2012) 4312–4319.
[31] R. Devi, S. Yadav, C.S. Pundir, Amperometric determination of xanthine in fish meat by zinc oxide nanoparticle/chitosan/multiwalled carbon nanotube/polyaniline composite film bound xanthine oxidase, Analyst 137 (2012) 754–759.
[32] D. Geng, S. Yang, Y. Zhang, J. Yang, J. Liu, R. Li, T. Sham, X. Sun, S. Ye, S. Knights, Nitrogen doping effects on the structure of graphene, Appl. Surf. Sci. 257 (2011) 9193–9198.
[33] R.C. Carvalho, C. Gouveia-Caridade, C.M.A. Brett, Glassy carbon electrodes modified by multiwalled carbon nanotubes and poly(neutral red). A comparative study of different brands and application to electrocatalytic ascorbate determination, Anal. Bioanal. Chem. 398 (2010) 1675–1685.
[34] S. Kakhki, M.M. Barsan, E. Shams, C.M.A. Brett, New robust redox and conducting polymer modified electrodes for ascorbate sensing and glucose biosensing, Electroanalysis 25 (2013) 77–84.
[35] C. Xian Guo, C.M. Li, Direct electron transfer of glucose oxidase and biosensing of glucose on hollow sphere-nanostructured conducting polymer/metal oxide composite, Phys. Chem. Chem. Phys. 12 (2010) 12153–12159.
[36] A.C. Conway, R.N. Goyal, G. Dryhurst, Electrochemical oxidation of hypoxanthine, J. Electroanal. Chem. 123 (1981) 243–264.
[37] G. Dryhurst, Electrochemical oxidation of uric-acid and xanthine at pyrolytic-graphite electrode – mechanistic interpretation of electrochemistry, J. Electrochem. Soc. 119 (1972) 1659–1664.
[38] R. Hille, Structure and function of xanthine oxidoreductase, Eur. J. Inorg. Chem. (2006) 1913–1926.
[39] K. Okamoto, T. Kusano, T. Nishino, Chemical nature and reaction mechanisms of the molybdenum cofactor of xanthine oxidoreductase, Curr. Pharm. Des. 19 (2013) 2606–2614.
[40] A.J. Clifford, D.L. Story, Levels of purines in foods and their metabolic effects in rats, J. Nutr. 106 (1976) 435–442.

Biographies

Madalina Maria Barsan received her PhD degree at University of Coimbra, Portugal, in 2011, where she is currently a postdoctoral researcher. Her research interests include the development of new nanostructured electrode materials and methods for biomolecule immobilization for application in biosensors and analytical chemistry.

Krishna P. Prathish received his PhD in chemistry at University of Kerala, India, in 2011 and is currently a postdoctoral researcher in the University of Coimbra, Portugal. His research interests include development of electrochemical/optical (bio) sensors, molecular imprinted polymers and analytical chemistry.

Xueliang Sun is a Canada Research Chair and professor at the University of Western Ontario, Canada. His current research interests are associated with synthesis of nanomaterials for electrochemical energy storage and conversion including fuel cells, lithium ion batteries and Li-air batteries.

Christopher Brett is a professor of chemistry at the University of Coimbra, Portugal. His research interests include new nanostructured electrode materials and modified electrode surfaces, electrochemical sensors and biosensors, electroactive polymers, corrosion and its inhibition, and applications of electrochemistry in the environmental, food and pharmaceutical areas.